Moulds, Rebecca J.; Buntine, Mark Anthony; Lawrance, Warren D.
Ab initio calculations of stationary points on the benzene-Ar and p-difluorobenzene-Ar potential energy surfaces: barriers to bound orbiting states, *Journal of Chemical Physics*, 2004; 121 (10):4635-4641.

Ab initio calculations of stationary points on the benzene–Ar and *p*-difluorobenzene–Ar potential energy surfaces: barriers to bound orbiting states

Rebecca J. Moulds
School of Chemistry, Physics and Earth Sciences, Flinders University, GPO Box 2100, Adelaide, South Australia 5001, Australia

Mark A. Buntine
Department of Chemistry, University of Adelaide, Adelaide, South Australia 5005, Australia

Warren D. Lawrance[a)]
School of Chemistry, Physics and Earth Sciences, Flinders University, GPO Box 2100, Adelaide, South Australia 5001, Australia

(Received 12 March 2004; accepted 20 May 2004)

The potential energy surfaces of the van der Waals complexes benzene–Ar and *p*-difluorobenzene–Ar have been investigated at the second-order Møller–Plesset (MP2) level of theory with the aug-cc-pVDZ basis set. Calculations were performed with unconstrained geometry optimization for all stationary points. This study has been performed to elucidate the nature of a conflict between experimental results from dispersed fluorescence and velocity map imaging (VMI). The inconsistency is that spectra for levels of *p*-difluorobenzene–Ar and –Kr below the dissociation thresholds determined by VMI show bands where free *p*-difluorobenzene emits, suggesting that dissociation is occurring. We proposed that the bands observed in the dispersed fluorescence spectra are due to emission from states in which the rare gas atom orbits the aromatic chromophore; these states are populated by intramolecular vibrational redistribution from the initially excited level [S. M. Bellm, R. J. Moulds, and W. D. Lawrance, J. Chem. Phys. **115**, 10709 (2001)]. To test this proposition, stationary points have been located on both the benzene–Ar and *p*-difluorobenzene–Ar potential energy surfaces (PESs) to determine the barriers to this orbiting motion. Comparison with previous single point CCSD(T) calculations of the benzene–Ar PES has been used to determine the amount by which the barriers are overestimated at the MP2 level. As there is little difference in the comparable regions of the benzene–Ar and *p*-difluorobenzene–Ar PESs, the overestimation is expected to be similar for *p*-difluorobenzene–Ar. Allowing for this overestimation gives the barrier to movement of the Ar atom around the *p*DFB ring via the valley between the H atoms as $\leqslant 204$ cm^{-1} in S_0 (including zero point energy). From the estimated change upon electronic excitation, the corresponding barrier in S_1 is estimated to be $\leqslant 225$ cm^{-1}. This barrier is less than the 240 cm^{-1} energy of $\overline{30^2}$, the vibrational level for which the anomalous ''free *p*-difluorobenzene'' bands were observed in dispersed fluorescence from *p*-difluorobenzene–Ar, supporting our hypothesis for the origin of these bands. © *2004 American Institute of Physics.* [DOI: 10.1063/1.1772355]

I. INTRODUCTION

Recently, we reported the results of velocity map imaging (VMI) measurements of the dissociation energies of the *p*-difluorobenzene–Ar (*p*DFB–Ar) and *p*-difluorobenzene–Kr (*p*DFB–Kr) van der Waals complexes.[1] These results conflict with observations made using dispersed fluorescence from vibrational levels in the S_1 state.[2,3] Dispersed fluorescence spectra from levels below the dissociation threshold determined by velocity map imaging (VMI) show bands at the position of free *p*DFB, suggesting that dissociation is occurring from these levels. Since this is not possible, the issue is why emission from the van der Waals complex appears at the free monomer position rather than at the usual spectroscopic shift (e.g., -30 cm^{-1} for *p*DFB–Ar). We postulated[1] that intramolecular vibrational energy redistribution (IVR) takes the complex from the initially excited level to states above the barrier to the rare gas atom moving from above the ring to below it. Once above this barrier, the rare gas atom can ''orbit'' the aromatic. We further postulate that emission from these bound ''orbiting'' states occurs at the position of free *p*DFB bands.

This explanation allows the VMI and dispersed fluorescence results to be reconciled provided both postulates are correct. First, the barriers to ''orbiting'' states must be below the vibrational states for which the ''free *p*DFB'' bands appear in the dispersed fluorescence spectra. Second, fluorescence from ''orbiting'' states must be shifted so as to be consistent with the experimental observations. In this paper we address the first issue through a series of *ab initio* calculations designed to determine the stationary points on the

a)Author to whom correspondence should be addressed. Electronic mail: warren.lawrence@flinders.edu.au

*p*DFB–Ar potential energy surface (PES), in particular the barrier to ''orbiting'' states. This is a necessary precursor to developing sufficiently detailed PESs that the vibrational states and, subsequently, emission spectra can be calculated for states above the barrier.

There have been few previous *ab initio* calculations reported for *p*DFB–Ar. However, there are extensive calculations available for the closely related benzene–Ar complex as this system has been the subject of increasingly advanced theoretical studies for more than a decade. The first *ab initio* calculations of benzene–Ar were reported by Hobza and coworkers who evaluated the geometry and binding energy of the complex at the MP2 level using a 6-31+G* basis set to describe the π system and $[7s4p2d]$ and $[7s4p2d1f]$ bases for the argon atom.[4] The ground electronic state binding energy was calculated to be 429 cm^{-1} (measured from the bottom of the potential well) while the benzene experimental geometry was kept rigid. Bludsky *et al.* examined the efficacy of two different empirical potentials in describing the vibrational dynamics of the benzene–Ar complex.[5] They found that the intermolecular vibrational levels were better described by a Morse-type potential than by a modified Lennard-Jones-type potential. Klopper *et al.* further investigated the benzene–Ar van der Waals complex by performing MP2–R12 calculations with a large basis set and found $D_e^0 = 553\,cm^{-1}$ (i.e., measured from the bottom of the potential well).[6] The benzene bond lengths R_{CC} and R_{CH} were kept fixed at 1.388 and 1.071 Å, respectively, in this study. More recently, high level *ab initio* calculations have been performed on the benzene–Ar ground (S_0) and excited state (S_1) intermolecular potential energy surfaces using the CCSD(T) method with a large basis set of QZ quality including midbond functions.[7,8] The experimentally determined benzene geometry was kept rigid during this study. Using these advanced *ab initio* methods, the authors determined the S_0 and S_1 binding energies, measured from the bottom of the potential well, to be 387 and 415 cm^{-1}, respectively. The most recent study is by Tarakeshwar and co-workers who performed an unrestricted optimization of the complex and report an MP2/aug-cc-pVDZ S_0 binding energy of 365 cm^{-1} (measured from the bottom of the potential well).[9] An experimental value of 314 ± 7 cm^{-1} has recently been reported for the binding energy, which includes zero point energy.[10] Comparison with the theoretical values given above requires adding the experimental zero point energy, determined from the frequencies of the van der Waals modes, of 53 cm^{-1}.[11,12]

For *p*DFB–Ar, early calculations were performed by Hobza *et al.* at the MP2 level with a 6-31+G* basis set for *p*DFB and a $[7s4p2d]$ basis set for Ar. These yielded an S_0 binding energy of 342 cm^{-1} (measured from the bottom of the potential well).[13] Most recently, Tarakeshwar *et al.* used the MP2/aug-cc-pVDZ method to calculate an S_0 binding energy of 349 cm^{-1} (measured from the bottom of the potential well).[9] The reported experimental value for the binding energy is 339 ± 4 cm^{-1}.[14] The experimental value for the zero-point energy, obtained from the frequencies of the van der Waals modes, is 41 cm^{-1}.[2,3]

We report here the results of calculations of the benzene–Ar and *p*DFB–Ar complexes using second-order Møller–Plesset (MP2) theory with an augmented correlation-consistent VDZ basis set. As the major attractive component of these interactions is dispersive in nature, a correlated level of theory is required to accurately describe the interaction of the inert rare gas with the π-electron cloud of the aromatic.[15] This combination was chosen to allow unconstrained optimizations to be performed at the various stationary points. We note that this is the first report of unconstrained optimization of stationary points, beyond the global minimum, for both the benzene–Ar and *p*DFB–Ar PESs.

With the computational resources available, it was not practical to run the required unconstrained calculations at the CCSD(T) level. Our strategy has been to perform the benzene–Ar calculations to provide a comparison with published single point CCSD(T) calculations, thereby giving an indication of likely overestimates in binding energies and barrier heights for the *p*DFB–Ar case.

II. COMPUTATIONAL METHODS

All calculations were performed using the GAUSSIAN 98 suite of programs at the MP2 level of theory, with Dunning's in-built aug-cc-pVDZ basis set.[16] The post-HF calculations employed the frozen core approximation whereby nonvalance, inner shell electrons were excluded from the Møller–Plesset correlation energy corrections.

Stationary points on each reaction potential energy surface were characterized as being minima or transition states by diagonalising the second-derivative Hessian matrix to determine the number of negative eigenvalues (0 for minima, 1 for transition states). All reported zero-point energies are scaled by 0.9343.[17]

In order to verify that the transition states identified connect to the expected minima, intrinsic reaction coordinate (IRC) calculations were performed, in which the paths of steepest descent (in mass-weighted Cartesian coordinates) were followed from each transition state to the connecting minima.[18] The default step size along the reaction path was 0.1 $amu^{1/2}$ bohr.

III. RESULTS FOR BENZENE–ARGON

Figure 1 details the coordinate system used to specify the position of the Ar atom relative to the aromatic ring. The position of the rare gas atom is indicated by a set of spherical polar coordinates (R_{vdW}, θ, ϕ), where R_{vdW} represents the equilibrium intermolecular van der Waals distance between the aromatic molecule center of mass and the Ar atom, and θ and ϕ describe the bending in the two planes perpendicular to the aromatic ring and internal rotation in the aromatic plane, respectively. In the coordinate system, the *z* axis lies along the C_6 symmetry axis and the *x*-axis passes through the carbon nuclei. The *y* axis is orthogonal to these and bisects the C–C bond.

The optimized benzene–Ar structures are shown in Fig. 2. In Table I we report the total energy, scaled zero-point energy (ZPE), relative energy including and excluding ZPE, and selected geometric parameters for each stationary point. A complete list of calculated (unscaled) vibrational frequen-

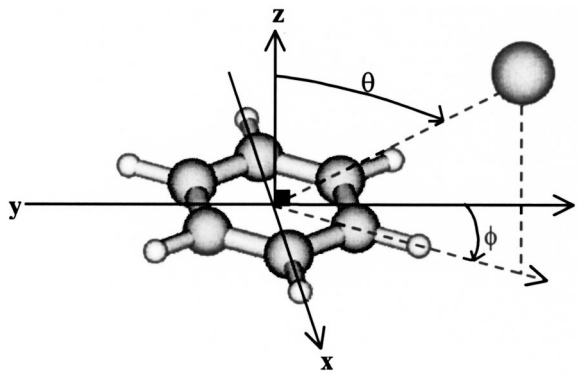

FIG. 1. The coordinate system used to specify the position of the Ar atom relative to the aromatic ring. The position of the rare gas atom is indicated by a set of spherical polar coordinates $(R_{\mathrm{vdW}},\theta,\phi)$, where R_{vdW} represents the equilibrium intermolecular van der Waals distance between the aromatic molecule center of mass and the Ar atom, and θ and ϕ describe the bending in planes perpendicular to the aromatic ring and internal rotation in the aromatic plane, respectively. The *z* axis lies along the C_6 symmetry axis and the *x*-axis passes through the carbon nuclei. The *y* axis is orthogonal to these and bisects the C–C bond.

cies and structural information for each stationary point is available as supplementary information.[19] The calculated benzene geometry is the same within the limits of the method at each stationary point, indicating that the position of the Ar atom has negligible structural affect on the aromatic molecule.

The benzene–Ar PES has two equivalent minima of C_{6v} symmetry, corresponding to the Ar atom located above the center of the benzene ring (one minimum above the benzene plane and one below it). This structure arises from the interaction between the Ar atom and the π-system of the benzene ring, and has previously been confirmed by theory[5,6] and experiment[20,21] to be the global minimum. The benzene–Ar S_0 binding energy (measured from the bottom of the well) is calculated to be 590 cm^{-1} with a corresponding R_{vdW} of 3.393 Å. The counterpoise method of Boys and Bernardi[22] was used to remove the basis set superposition error (BSSE),

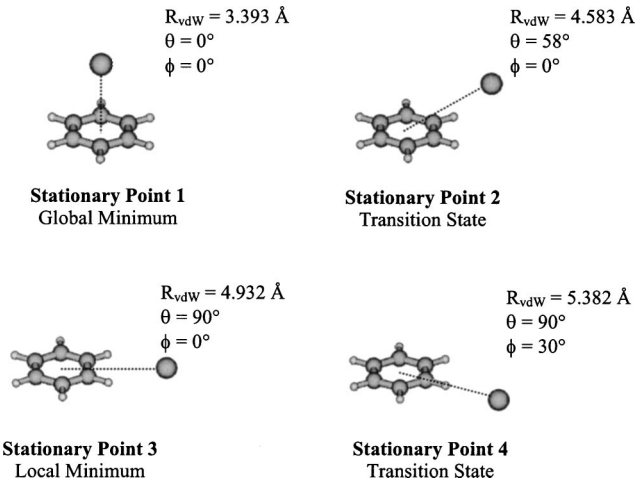

FIG. 2. The optimized structures for the stationary points on the benzene–Ar PES. Table I gives the total energy, scaled zero-point energy (ZPE), relative energy including and excluding ZPE, and selected geometric parameters for each stationary point.

TABLE I. The MP2/aug-cc-pVDZ total energy, scaled zero-point energy (ZPE), relative energy, and selected geometric parameters for each stationary point on the benzene–Ar potential energy surface.[a]

Stationary point	Total energy	ZPE	Relative energy	R_{vdW}	θ	ϕ
Global minimum (1)	−758.498 20	0.093 09	0	3.393	0	0
Transition state (2)	−758.497 08	0.093 04	235	4.583	58	0
Local minimum (3)	−758.497 35	0.093 07	184	4.932	90	0
Transition state (4)	−758.496 76	0.093 07	314	5.382	90	30

[a]Total energies are in hartrees. ZPEs are in hartrees/particle. Relative energies are in cm^{-1}. Distances are in Å. Angles are in degrees. Optimized benzene geometry for each stationary point: $R_{\mathrm{CC}}=1.408$ Å, $R_{\mathrm{CH}}=1.094$ Å, $R_{\mathrm{CH(Ar)}}=1.093$ Å (for stationary point 4 only).

leading to a corrected binding energy of 375 cm^{-1}. This value agrees favorably with the MP2/aug-cc-pVDZ results of Tarakeshwar *et al.* who report a BSSE corrected binding energy of 365 cm^{-1} and a R_{vdW} of 3.364 Å.[9] The binding energy is the only value for which BSSE corrections are reported.

Comparison with the experimentally determined binding energy requires accounting for zero point energy (ZPE). We calculate the benzene–Ar ZPE correction to be 66 cm^{-1} and inclusion of this results in a final S_0 binding energy of 309 cm^{-1}. This calculated value is remarkably similar to the experimentally determined S_0 binding energy of 314 ± 7 cm^{-1}.[10] It has previously been shown that MP2/aug-cc-pVDZ calculations accurately reproduce the complex properties due to a fortuitous cancellation of basis set and correlation errors.[15]

The calculated equilibrium intermolecular separation is ~0.19 Å smaller than the experimental value of 3.582 Å (Ref. 20) due to the fact that the complex geometries also suffer from BSSEs.[9,15] The computational effort required to remove this error is considerable and as our uncorrected geometry compares well with those previously reported, the geometry corrections were not performed.

Six equivalent very flat minima, located in the benzene plane, arise from the interaction of the Ar atom with pairs of benzene H atoms. The energy of these minima is 184 cm^{-1} above the global minimum, including ZPE. The barrier to movement of Ar from the global minimum to the in-plane minimum is 235 cm^{-1} (including ZPE). Thus the barrier to Ar switching from above the benzene plane, through the in-plane minimum, to the equivalent position below the plane (and vice versa) is calculated to be 235 cm^{-1}. A pictorial summary of the benzene–Ar PES for movement of the Ar atom around the benzene ring is presented in Fig. 3. The in-plane motion of the Ar atom around the benzene ring was also explored and the barrier to movement between the in-plane local minima is found to be 314 cm^{-1} (including ZPE). This transition state corresponds to the Ar atom in line with a C–H bond.

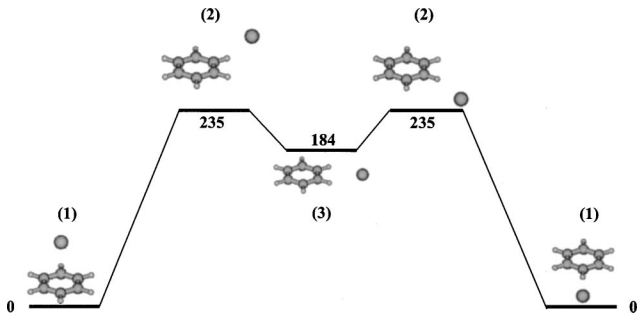

FIG. 3. A pictorial summary of the stationary points on the benzene–Ar PES for movement of the Ar atom from one face of the benzene ring to the other via the lowest energy pathway.

IV. RESULTS FOR *p*-DIFLUOROBENZENE–ARGON

Earlier experimental and theoretical studies of the closely related π–Ar systems benzene–Ar, fluorobenzene–Ar, and *p*-difluorobenzene–Ar have shown that the presence of the electron-withdrawing fluorine has little effect on the binding energy of these complexes.[9,10,13,14,23,24] Consequently, there is expected to be very little difference between the benzene–Ar and *p*DFB–Ar PESs, as far as the interaction with the π-system and C–H regions of the PES are concerned.

The axis system for *p*DFB–Ar is essentially the same as that used for benzene–Ar. The value $\phi=0$ corresponds to the Ar atom lying in the plane perpendicular to the aromatic that bisects the C–C bond of the carbon atoms bonding to H; when $\phi=90°$ the Ar atom lies in the plane that is perpendicular to the aromatic and contains the C–F bonds.

Seven stationary points were located on the *p*DFB–Ar PES. The optimized structures are shown in Fig. 4. In Table II we report the total energy, scaled zero-point energy, relative energy including and excluding ZPE, and selected geometric parameters for each stationary point. A complete list of calculated (unscaled) vibrational frequencies and structural information for each stationary point is available as supplementary information.[19]

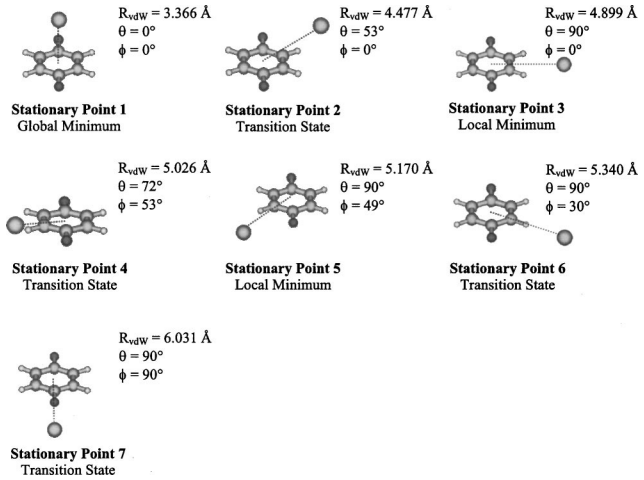

FIG. 4. The optimized structures for the seven stationary points located on the *p*DFB–Ar PES. The total energy, scaled zero-point energy, relative energy including and excluding ZPE, and selected geometric parameters for each stationary point are given in Table II.

TABLE II. The MP2/aug-cc-pVDZ total energy, scaled zero-point energy (ZPE), relative energy, and selected geometric parameters for each stationary point on the *p*-difluorobenzene–Ar potential energy surface.[a]

	Total energy	ZPE	Relative energy	R_{vdW}	θ	ϕ
Global minimum (1)	−956.614 19	0.078 16	0	3.366	0	0
Transition state (2)	−956.612 93	0.078 06	255	4.477	53	0
Local minimum (3)	−956.613 26	0.078 19	211	4.899	90	0
Transition state (4)	−956.612 83	0.078 06	275	5.026	72	53
Local minimum (5)	−956.612 87	0.078 20	300	5.170	90	49
Transition state (6)	−956.612 75	0.078 19	324	5.340	90	30
Transition state (7)	−956.612 18	0.078 03	414	6.031	90	90

[a]Total energies are in hartrees. ZPEs are in hartrees/particle. Relative energies are in cm^{-1}. Distances are in Å. Angles are in degrees. Optimized *p*DFB geometry for each stationary point: $R_{CC(HH)}=1.407$ Å, $R_{CC(HF)}=1.399$ Å, $R_{CH}=1.092$ Å, $R_{CF}=1.368$ Å.

As with the benzene–Ar complex, the Ar atom is located directly over the center of the aromatic ring in the lowest energy structure. The *p*DFB–Ar S_0 binding energy, calculated from the bottom of the well, is determined to be 633 cm^{-1}. As for benzene–Ar, the counterpoise method was used to remove BSSE, leading to a corrected S_0 binding energy of 377 cm^{-1}. Inclusion of the calculated ZPE of 56 cm^{-1} leads to a final S_0 binding energy of 321 cm^{-1}. This value is similar to the calculated benzene–Ar S_0 binding energy of 309 cm^{-1} reported above. It agrees favorably with the experimental value of 339 ± 4 cm^{-1} for *p*DFB–Ar.[14] As for benzene–Ar, the binding energy is the only value for which BSSE corrections are reported.

A slight decrease in the equilibrium intermolecular separation is observed with addition of the F substituent. The van der Waals equilibrium bond length is calculated to be 3.366 Å, which is a decrease of 0.027 Å compared with benzene–Ar. Tarakeshwar *et al.* report a similar decrease of 0.029 Å using the same method.[9] It has been shown that the geometry and stability of aromatic-rare gas van der Waals complexes are determined by a balance between the stabilizing dispersion interactions and destabilizing exchange–repulsion interactions.[9,15] The presence of the electron-withdrawing fluorine contracts the π-density above and below the ring towards the carbon atoms, reducing the exchange–repulsion component and increasing the dispersion interactions. This allows for a closer approach of the Ar atom to the substituted aromatic, while the overall energetics of the system remain largely unperturbed.

The presence of the F substituent on the *p*DFB ring results in two distinctly different in-plane local minima, involving Ar binding in a bridge configuration to either two hydrogens or to a hydrogen and a fluorine. For clarity, we refer to these in-plane minima as the H–H and H–F minima,

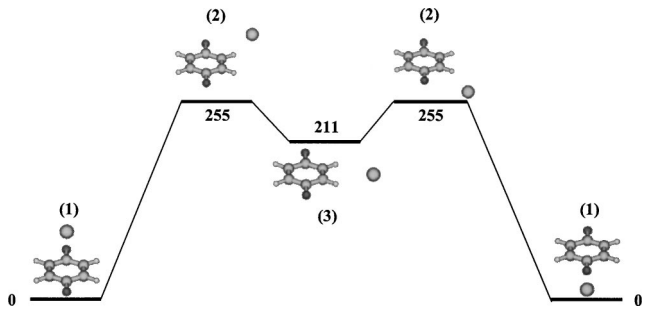

FIG. 5. A pictorial summary of the stationary points on the *p*DFB–Ar PES for movement of the Ar atom from one face of the *p*DFB ring to the other via the lowest energy pathway.

respectively. Including the ZPE, these local minima are 211 and 300 cm^{-1} higher in energy than the global minimum, respectively. The movement of the Ar atom from above the center of the ring to the H–H minimum occurs over a barrier of 255 cm^{-1} (including ZPE). Thus the lowest barrier for movement of the Ar from one side of the *p*DFB chromophore to the other involves a 255 cm^{-1} barrier. A pictorial summary of the lowest energy pathway is presented in Fig. 5.

When the ZPE correction terms are not included, a barrier of 298 cm^{-1} exists between the global minimum and the H–F minimum. The H–F minimum is only 9 cm^{-1} lower in energy than the related transition state. The zero-point energy for the transition structure is less than that for the minimum due to the exclusion of the unbound frequency and, as a result, we find that this barrier disappears when ZPE is included. Consequently, the H–F minimum can be considered the transition state for movement of the Ar atom around the *p*DFB ring this way, with the barrier calculated to be 300 cm^{-1}.

Two transition structures were located for the in-plane movement of the Ar around the *p*DFB ring. The movement over the H atom was found to be lower in energy (324 cm^{-1}) than movement over the F atom (414 cm^{-1}). The corresponding barrier for in-plane movement of the Ar over a H atom is 314 cm^{-1} for benzene indicating, as expected, little change on fluorination. Both in-plane barriers are considerably elevated compared with that for movement of the Ar from the global to in-plane minima.

V. DISCUSSION

Comparisons with the results of previous calculations have been made during the presentation of the results and we focus in this section on the insights into the barriers to ''orbiting'' motion gleaned from the calculations. It will be recalled that the calculations were aimed at testing the hypothesis that bands previously assigned to free *p*DFB in dispersed fluorescence spectra from the $\overline{30^2}$ level of the *p*DFB–Ar complex are due to emission from states in which the Ar atom orbits the aromatic chromophore.

As discussed in Sec. IV, our calculations predict the lowest barrier for movement of the Ar from one side of the *p*DFB chromophore to the other to involve a 255 cm^{-1} barrier (including ZPE). Given that the interaction is strengthened in the S_1 state, a higher barrier is expected in S_1, which is the state relevant to the experiments. The anomalous fluorescence bands are observed following excitation of $\overline{30^2}$, which has an energy of 240 cm^{-1}. Thus at first glance it appears that the calculations rule out the possibility of orbiting states being accessible following excitation of $\overline{30^2}$. However, our calculations have been performed at the MP2 level and are expected to provide upper bounds to the barrier heights, i.e., they will overestimate the barrier heights. Consequently, our strategy has been to perform calculations for the closely related benzene–Ar complex for which single point CCSD(T) calculations have been performed for both the S_0 and S_1 electronic states. Although these calculations were performed without geometry optimization, they are expected to yield more reliable values than those performed at the MP2 level. A comparison between our calculations and the CCSD(T) results should provide an indication of the degree to which the barrier is overestimated in the *p*DFB–Ar case and allow us to determine a reasonable value for this barrier.

Comparison of the relative energies of the benzene–Ar stationary points calculated at the MP2 level in this study with those previously reported at the CCSD(T) level reveals, as expected, that the MP2 barriers are higher than those calculated at the higher level of theory.[7] In their study of the S_0 and S_1 states of benzene–Ar, Koch *et al.* found that the differences between MP2 and CCSD(T) level binding energies were stable with respect to increasing basis set size.[25] Our MP2 level calculations determine the height of the barrier for motion of the Ar from one face of the aromatic to the other to be (excluding ZPE) 31 cm^{-1} higher for *p*DFB–Ar compared with benzene–Ar. Thus we can infer that the CCSD(T) *p*DFB–Ar barrier will be approximately 31 cm^{-1} higher than that found for benzene–Ar using the same level of theory. The reported CCSD(T) value for the S_0 benzene–Ar barrier height is 184 cm^{-1}, excluding ZPE. Therefore the S_0 *p*DFB–Ar barrier is expected to be ~215 cm^{-1}. Since the CCSD(T) calculations did not include geometry optimization, they provide an upper limit to the barrier height (the relaxation of the geometry to the minimum must lower the energy), suggesting that the value of 215 cm^{-1} is likely to be an upper limit to the true barrier. The inclusion of ZPE reduces the barrier height due to the exclusion of the unbound frequency at the barrier. With ZPE included the S_0 *p*DFB–Ar barrier is predicted to be $\leqslant$204 cm^{-1}.

To determine whether the barrier to the Ar orbiting the *p*DFB lies below the states for which ''free *p*DFB'' bands appear in the dispersed fluorescence spectra, we need to examine the barrier in the excited state of the complex. The CCSD(T) calculations of the benzene–Ar S_0 and S_1 PESs predict that the S_1 well is deeper than that of S_0 by 28.1 cm^{-1} and, with ZPE included, the spectral shift upon electronic excitation is calculated to be -16 cm^{-1}.[8] This compares very well with the experimental value of -21 cm^{-1},[26] giving us faith in the CCSD(T) level predictions of changes upon electronic excitation. The CCSD(T) calculations show the barrier to movement of the Ar atom from one face of benzene to the other increases by 21 cm^{-1} upon electronic excitation, excluding ZPE.[8] A similar increase is also re-

ported for the in-plane minimum. We have noted above the similarities between the *p*DFB–Ar and benzene–Ar PESs as far as the π-system and C–H regions are concerned. It is thus not unreasonable to expect a similar increase in barrier heights between S_0 and S_1 for the two species. The barrier for movement of the Ar atom from one face of the *p*DFB ring to the other in S_1 is thus estimated to be 236 cm^{-1} or less, excluding ZPE. Including ZPE lowers the barrier by 11 cm^{-1} in S_0. The *p*DFB–Ar ZPE in S_1 is larger than that in S_0 due to an increase in the frequency of the bending modes (17 and 23 cm^{-1} in S_0 compared with 25 and 34 cm^{-1} in S_1, for the long and short in-plane bending modes, respectively).[2,27] Consequently, the barrier height will be reduced by slightly more than 11 cm^{-1} in S_1. We conclude that the inclusion of ZPE will result in a barrier of 225 cm^{-1} or less in S_1.

In dispersed fluorescence from *p*DFB–Ar, bands are observed where free *p*DFB emits following excitation of the $\overline{30^2}$ vibrational level ($E_{vib}=240\,cm^{-1}$).[1–3] Since the dissociation energy of 369 ± 4 cm^{-1} determined from VMI experiments is greater than the vibrational energy of $\overline{30^2}$,[1,14] free *p*DFB cannot be formed following excitation of this level. We suggested that these observations might be reconciled if the barrier to the Ar atom orbiting the *p*DFB moiety lies below the $\overline{30^2}$ energy, i.e., is <240 cm^{-1}. By taking into account the overestimation of the MP2 method when compared with CCSD(T) calculations and the estimated shift on electronic excitation, the barrier to movement of the Ar atom around the *p*DFB ring is estimated to be $\leqslant 255$ cm^{-1}. The calculations indicate that the first assumption of our hypothesis for the origin of the bands seen in the dispersed fluorescence spectrum is correct, although it appears likely that the barrier lies not far below the $\overline{30^2}$ energy. Given the closeness of the expected barrier to the $\overline{30^2}$ energy, it would appear necessary to undertake CCSD(T) level calculations on the S_1 state of *p*DFB–Ar to fully resolve this issue.

The calculations of the benzene–Ar surface provide an interesting prediction for the behavior of this molecule. Should our hypothesis concerning orbiting states be correct, the anomalous fluorescence behavior observed for *p*DFB–Ar and *p*DFB–Kr should be a general feature of aromatic-rare gas complexes. The benzene–Ar binding energy has recently been reported as 335 cm^{-1} in S_1.[10] The first major absorption feature in the $S_1 \leftarrow S_0$ spectrum is $\overline{6^1_0}$, which produces the complex with 521 cm^{-1} of vibrational energy. The lowest S_1 vibrational level is $\overline{16^1}$, with an energy of 237 cm^{-1}. Excitation of $\overline{6^1}$ can lead to dissociation of the complex but the only product state accessible is 0^0. However, IVR from $\overline{6^1}$ can produce the complex in the $\overline{16^1}$ state with sufficient energy in van der Waals modes to be above the barrier to the Ar atom moving from one face of the aromatic ring to the other. Thus we predict that, following excitation of $\overline{6^1}$, emission from $\overline{16^1}$ will appear 21 cm^{-1} to the blue of its expected position, i.e., at the position of emission from 16^1 benzene. This gives an interesting test of our hypothesis for the influence of orbiting states on the spectra of van der Waals molecules.

VI. SUMMARY AND CONCLUSIONS

We have used the MP2/aug-cc-pVDZ method to examine the geometry, binding energy, and stationary points on the benzene–Ar and *p*DFB–Ar potential energy surfaces. The calculations were undertaken with unconstrained geometry optimization. The benzene–Ar S_0 binding energy is calculated to be 309 cm^{-1} (including ZPE) at an equilibrium intermolecular separation of 3.393 Å. Four stationary points were located on the PES corresponding to the C_{6v} global minimum, a local in-plane minimum, and the two (equivalent) transition structures for movement between these two minima. The barrier to movement of the Ar atom from the global minimum above the benzene plane to the equivalent position below the plane (and vice versa) is calculated to be 235 cm^{-1}, including ZPE. The binding energy and geometry agree well with those previously reported using the same method, and the calculated binding energy is very similar to the experimental value.

The *p*DFB–Ar S_0 binding energy is calculated to be 321 cm^{-1} with a corresponding equilibrium intermolecular separation of 3.366 Å. Again, these results agree favorably with those previously reported and the binding energy is comparable with the experimentally determined S_0 value of 339 cm^{-1}. Seven stationary points were located on the *p*DFB–Ar PES corresponding to the C_{2v} global minimum, two in-plane local minima (one involving the Ar bridging to the two hydrogens and the other involving the Ar bridging to a hydrogen and a fluorine), and four transition structures connecting these minima. Movement of the Ar from one side of the *p*DFB ring to the other through the two local in-plane minima was investigated. The lowest energy path was found to be between two hydrogen atoms with a barrier of 255 cm^{-1}.

The calculated barrier to movement of the Ar atom around the *p*DFB ring is 31 cm^{-1} higher in energy than the corresponding barrier in benzene–Ar. Comparison of the MP2 level barriers for benzene–Ar with single point CCSD(T) level calculations indicates that the MP2 barrier heights are overestimated. By allowing for this overestimation, as well as the reduction in barrier height upon inclusion of zero-point energy, we estimate that at the CCSD(T) level of theory the barrier for *p*DFB–Ar will be $\leqslant 204$ cm^{-1}. CCSD(T) calculations of benzene–Ar show that this barrier will increase upon electronic excitation. The barrier to movement of the Ar atom around the *p*DFB ring in S_1 is estimated to be $\leqslant 225$ cm^{-1}. This is below the vibrational level from which anomalous fluorescence is observed ($E_{vib}=240\,cm^{-1}$), suggesting that upon excitation of this vibrational level, fluorescence can occur from ''orbiting states'' where the Ar is free to move around the aromatic chromophore. However, given the closeness of the expected barrier to the $\overline{30^2}$ energy, it would appear necessary to undertake CCSD(T) level calculations on the S_1 state of *p*DFB–Ar to fully resolve this issue.

ACKNOWLEDGMENTS

This work was undertaken with the financial support of the Australian Research Council and Flinders University.

Computing resources provided by the Australian Partnership for Advanced Computing (APAC) and the South Australian Center for Parallel Computing (SACPC). R.J.M. thanks the Australian Government for financial support through an Australian Postgraduate Award.

APPENDIX: SUPPORTING INFORMATION AVAILABLE

Supporting information has been provided as an EPAPS document. This supporting information gives a listing of complete geometry specifications (in Cartesian coordinates) for each stationary point on the potential energy surface of each complex, together with a full listing of unscaled vibrational frequencies. Details for accessing this information are given in Ref. 19.

[1] S. M. Bellm, R. J. Moulds, and W. D. Lawrance, J. Chem. Phys. **115**, 10709 (2001).
[2] M.-C. Su, H.-K. O, and C. S. Parmenter, Chem. Phys. **156**, 261 (1991).
[3] H.-K. O. , C. S. Parmenter, and M.-C. Su, Ber. Bunsenges. Phys. Chem. **92**, 253 (1988).
[4] P. Hobza, H. L. Selzle, and E. W. Schlag, J. Chem. Phys. **95**, 391 (1991).
[5] O. Bludsky, V. Spirko, V. Hrouda, and P. Hobza, Chem. Phys. Lett. **196**, 410 (1992).
[6] W. Klopper, H. P. Lüthi, Th. Brupbacher, and A. Bauder, J. Chem. Phys. **101**, 9747 (1994).
[7] H. Koch, B. Fernández, and J. Makarewicz, J. Chem. Phys. **111**, 198 (1999).
[8] B. Fernández, H. Koch, and J. Makarewicz, J. Chem. Phys. **111**, 5922 (1999).
[9] P. Tarakeshwar, K. S. Kim, E. Kraka, and D. Cremer, J. Chem. Phys. **115**, 6018 (2001).
[10] R. K. Sampson and W. D. Lawrance, Aust. J. Chem. **56**, 275 (2003).
[11] E. Riedle and A. van der Avoird, J. Chem. Phys. **104**, 882 (1996).
[12] Th. Brupbacher, J. Makarewicz, and A. Bauder, J. Chem. Phys. **101**, 9736 (1994).
[13] P. Hobza, H. L. Selzle, and E. W. Schlag, J. Chem. Phys. **99**, 2809 (1993).
[14] S. M. Bellm, J. R. Gascooke, and W. D. Lawrance, Chem. Phys. Lett. **330**, 103 (2000).
[15] J. J. Oh, I. Park, R. J. Wilson, S. A. Peebles, R. L. Kuczkowski, E. Kraka, and D. Cremer, J. Chem. Phys. **113**, 9051 (2000).
[16] M. J. Frisch, G. W. Trucks, H. B. Schlegel *et al.*, GAUSSIAN 98, Revision A.11.3, Gaussian, Inc., Pittsburgh, PA, 2002.
[17] J. B. Foresman and Æ. Frisch, *Exploring Chemistry with Electronic Structure Methods*, 2nd ed. (Gaussian Inc., Pittsburgh, PA, 1996).
[18] C. Ganzalez and H. B. Schlegel, J. Chem. Phys. **90**, 2154 (1989).
[19] See EPAPS Document No. E-JCPSA6-121-316430 for a listing of complete geometry specifications (in Cartesian coordinates) for each stationary point on the potential energy surface of each complex, together with a full listing of unscaled vibrational frequencies. A direct link to this document may be found in the online article's HTML reference section. The document may also be reached via the EPAPS homepage (http://www.aip.org/pubservs/epaps.html) or from ftp.aip.org in the directory /epaps/. See the EPAPS homepage for more information.
[20] Th. Weber, A. von Bargen, E. Riedle, and H. J. Neusser, J. Chem. Phys. **92**, 90 (1990).
[21] Th. Brupbacher and A. Bauder, Chem. Phys. Lett. **173**, 435 (1990).
[22] S. F. Boys and F. Bernardi, Mol. Phys. **19**, 553 (1970).
[23] Th. Grebner, P. V. Unold, and H. J. Neusser, J. Phys. Chem. A **101**, 158 (1997).
[24] G. M. Lembach and B. Brutschy, J. Chem. Phys. **107**, 6156 (1997).
[25] H. Koch, B. Fernández, and O. Christiansen, J. Chem. Phys. **108**, 2784 (1998).
[26] T. A. Stephenson and S. A. Rice, J. Chem. Phys. **81**, 1083 (1984).
[27] R. Sussman and H. J. Neusser, J. Chem. Phys. **102**, 3055 (1994).